J|A|C|S
ARTICLES
Published on Web 11/08/2006

Zinspy Sensors with Enhanced Dynamic Range for Imaging Neuronal Cell Zinc Uptake and Mobilization

Elizabeth M. Nolan,[†] Jubin W. Ryu,[§] Jacek Jaworski,[§,||,#] Rodney P. Feazell,[†] Morgan Sheng,[§,⊥,||] and Stephen J. Lippard*[,†]

Contribution from the Department of Chemistry, Picower Institute of Learning and Memory, RIKEN−MIT Neuroscience Research Center, and Howard Hughes Medical Institute, Massachusetts Institute of Technology, Cambridge, Massachusetts 02139, and Laboratory of Molecular and Cellular Neurobiology, International Institute of Molecular and Cell Biology, 02-109 Warsaw, Poland

Received August 9, 2006; E-mail: lippard@mit.edu

Abstract: Thiophene moieties were incorporated into previously described Zinspy (ZS) fluorescent Zn(II) sensor motifs (Nolan, E. M.; Lippard, S. J. *Inorg. Chem.* **2004**, *43*, 8310−8317) to provide enhanced fluorescence properties, low-micromolar dissociation constants for Zn(II), and improved Zn(II) selectivity. Halogenation of the xanthenone and benzoate moieties of the fluorescein platform systematically modulates the excitation and emission profiles, pH-dependent fluorescence, Zn(II) affinity, and Zn(II) complexation rates, offering a general strategy for tuning multiple properties of xanthenone-based metal ion sensors. Extensive biological studies in cultured cells and primary neuronal cultures demonstrate 2-{6-hydroxy-3-oxo-4,5-bis[(pyridin-2-ylmethylthiophen-2-ylmethylamino)methyl]-3*H*-xanthen-9-yl}benzoic acid (ZS5) to be a versatile imaging tool for detecting Zn(II) in vivo. ZS5 localizes to the mitochondria of HeLa cells and allows visualization of glutamate-mediated Zn(II) uptake in dendrites and Zn(II) release resulting from nitrosative stress in neurons.

Introduction

The neurobiology of zinc has attracted significant attention.[1,2] Zinc is the second most abundant d-block metal ion in the human brain, with relatively high concentrations found in the hippocampus and neocortex.[3] Of particular interest to this work is zinc found in the hippocampus, a region of the mammalian forebrain involved in learning and memory formation. This zinc can be divided into two types,[4] protein bound and loosely bound, the latter also termed histochemically observable, chelatable, or mobile.[5] Hippocampal loosely bound zinc is housed in the synaptic vesicles of glutamatergic mossy fiber neurons. Co-localization of zinc and glutamate in this subset of synaptic vesicles was assumed for decades, but proof of such mutual uptake was provided only recently.[6]

Many studies point to the importance of Zn(II) in human neurophysiology. Multiple neuromodulatory effects for Zn(II) have been documented and include down-regulation of *N*-methyl-D-aspartate receptors,[7−10] one major type of glutamatergic ion channel in the mammalian central nervous system, and inhibition of Ca(II) channels.[11] Zinc has also been implicated in long-term potentiation (LTP), an electrophysiological phenomenon thought to underlie certain forms of learning and memory, in DG → CA3 synapses.[12] Despite these observations, the concept of vesicular zinc release into the synapse remains controversial.[13−19]

Zinc pathology is also an area of current interest. High concentrations of Zn(II) are neurotoxic. A number of zinc transporter proteins[20,21] and metallothionein[22,23] maintain zinc homeostasis under normal physiological conditions, but these

[†] Department of Chemistry, MIT.
[§] Picower Institute of Learning and Memory, MIT.
[⊥] RIKEN−MIT Neuroscience Research Center.
[||] Howard Hughes Medical Institute.
[#] International Institute of Molecular and Cell Biology, Poland.

(1) Frederickson, C. J.; Koh, J.-H.; Bush, A. I. *Nat. Neurosci.* **2005**, *6*, 449−462.
(2) Chang, C. J.; Lippard, S. J. *Metal Ions Life Sci.* **2006**, *1*, 321−370.
(3) Frederickson, C. J. *Int. Rev. Neurobiol.* **1989**, *31*, 145−238.
(4) Takeda, A. *BioMetals* **2001**, *14*, 343−351.
(5) "Mobile" can also refer to zinc that has been released from native protein stores.
(6) Salazar, G.; Craige, B.; Love, R.; Kalman, D.; Faundez, V. *J. Cell Sci.* **2005**, *118*, 1911−1921.
(7) Peters, S.; Koh, J.; Choi, D. W. *Science* **1987**, *236*, 589−593.
(8) Kim, T.-Y.; Hwang, J. J.; Yun, S. H.; Jung, M. W.; Koh, J. Y. *Synapse* **2002**, *46*, 49−56.
(9) Molnár, P.; Nadler, J. V. *Brain Res.* **2001**, *910*, 205−207.
(10) Ueno, S.; Tsukamoto, M.; Hirano, T.; Kikuchi, K.; Yamada, M. K.; Nishiyama, N.; Nagano, T.; Matsuki, N.; Ikegaya, Y. *J. Cell Biol.* **2002**, *158*, 215−220.
(11) Davies, P. A.; Wang, W.; Hales, T. G.; Kirkness, E. F. *J. Biol. Chem.* **2003**, *278*, 712−717.
(12) Li, Y.; Hough, C. J.; Frederickson, C. J.; Sarvey, J. M. *J. Neurosci.* **2001**, *21*, 8015−8025.
(13) Assaf, S. Y.; Chung, S.-H. *Nature (London)* **1984**, *308*, 734−736.
(14) Howell, G. A.; Welch, M. G.; Frederickson, C. J. *Nature (London)* **1984**, *308*, 736−738.
(15) Li, Y.; Hough, C. J.; Suh, S. W.; Sarvey, J. M.; Frederickson, C. J. *J. Neurophysiol.* **2001**, *86*, 2597−2604.
(16) Kay, A. R. *J. Neurosci.* **2003**, *23*, 6847−6855.
(17) Qian, J.; Noebels, J. L. *J. Physiol.* **2005**, *566*, 747−758.
(18) Frederickson, C. J.; Giblin, L. J.; Rengarajan, B.; Masalha, R.; Frederickson, C. J.; Zeng, Y.; Lopez, E. V.; Koh, J.-Y.; Chorin, U.; Besser, L.; Herskfinkel, M.; Li, Y.; Thompson, R. B.; Krezel, A. *J. Neurosci. Methods* **2006**, *154*, 19−29.
(19) Kay, A. R. *Trends Neurosci* **2006**, *29*, 200−206.
(20) Liuzzi, J. P.; Cousins, R. J. *Annu. Rev. Nutr.* **2004**, *24*, 151−172.

mechanisms can fail during periods of stress. Uncontrolled zinc release occurs from protein-bound and vesicular stores following blunt head trauma and as a result of stroke or seizure, and it is implicated in subsequent neurodegeneration.[24−29] Evidence exists for a role of Zn(II) in the onset and pathogenesis of Alzheimer's disease.[30] There are several mechanisms to explain Zn(II) neurotoxicity, including rapid influx into mitochondria, which triggers apoptosis following uncontrolled release.[28,31] Of particular relevance to some of the work described here is the growing link between Zn(II) toxicity and oxidative stress.[27,31,32]

Despite this knowledge, many details regarding the functional significance of Zn(II) in neurobiology remain elusive. This situation has motivated the design of many new Zn(II) imaging tools suitable for studies in living cells. Initially, aryl sulfonamide-based sensors, including *N*-(6-methoxy-8-quinolyl)-*p*-toluenesulfonamide (TSQ) and its derivatives, were employed to visualize chelatable Zn(II) in the mammalian hippocampus and in live cells.[33−36] Over the past six years, in part guided by tactics used for Ca(II) sensing,[37] significant advances in biological Zn(II) sensor design have been made.[2,38−41] Many sensors, including the ACF,[42] ZnAF,[43,44] Fluo- and Rhod-Zn,[45,46] Zinpyr,[47−49] and QZ[50] probes, provide visible excitation and bright fluorescence in the Zn(II)-bound forms. Some of these sensors have been employed in studies of Zn(II) neurobiology.[17,44,49,50] Small-molecule ratiometric Zn(II) sensors have been documented,[46,51−55] several of which have been applied in vivo.[53,54] Protein-based[56−59] approaches have also emerged as useful Zn(II) sensing tools, and several peptide-based[60−62] strategies have been reported. Nevertheless, the design and implementation of new Zn(II) imaging reagents is required to continue advances in this field. Several recent initiatives[44,50,63] address the need for Zn(II) sensors with varying affinities for use in vivo, since estimated endogenous Zn(II) concentrations vary widely, depending on the tissue or cell type under study.

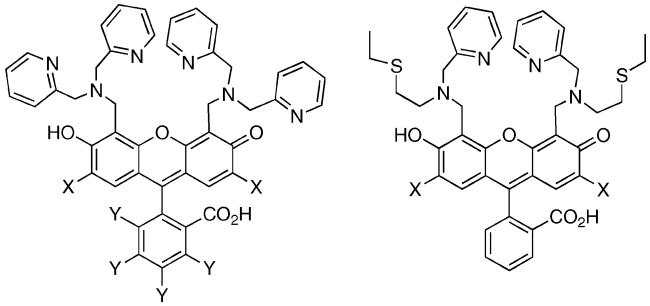

Figure 1. Symmetrical and tertiary-amine-based Zinpyr (ZP) and Zinspy (ZS) sensors.

We previously reported the Zinpyr (ZP)[47−49] and Zinspy (ZS)[64] families of Zn(II) sensors, several of which are depicted in Figure 1. The thioether-for-pyridyl substitution that gives the ZS sensors was made with the aims of lowering Zn(II) affinity and potentially modulating metal-ion selectivity relative to the parent ZP compounds, which employ the di(2-picolyl)amine (DPA) chelate. Although the ZS probes exhibit improved Zn(II) selectivity and lower affinity Zn(II) binding as compared to their DPA-based counterparts, they generally suffer from relatively poor photophysical properties, including high background fluorescence and weak (≤2-fold) fluorescence enhancement with Zn(II) coordination, at least for the tertiary amine-based systems. These features preclude facile application of these sensors for biological imaging of Zn(II).

In the present article, we describe Zinspy sensors with enhanced dynamic range. On the basis of several observations

(21) Colvin, R. A.; Fontaine, C. P.; Laskowski, M.; Thomas, D. *Eur. J. Pharmacol.* **2003**, *479*, 171−185.
(22) Ebadi, M.; Iversen, P. L.; Hao, R.; Cerutis, D. R.; Rojas, P.; Happe, H. K.; Murrin, L. C.; Pfeiffer, R. F. *Neurochem. Int.* **1995**, *27*, 1−22.
(23) Jacob, C.; Maret, W.; Vallee, B. L. *Proc. Natl. Acad. Sci. U.S.A.* **1998**, *95*, 3489−3494.
(24) Choi, D. W.; Koh, J. Y. *Annu. Rev. Neurosci.* **1998**, *21*, 347−375.
(25) Lee, J.-Y.; Cole, T. B.; Palmiter, R. D.; Koh, J.-Y. *J. Neurosci.* **2000**, *20*, RC79 1−5.
(26) Lee, J.-Y.; Kim, J.-H.; Palmiter, R. D.; Koh, J.-Y. *Exp. Neurol.* **2003**, *184*, 337−347.
(27) Wei, G.; Hough, C. J.; Sarvey, J. M. *Neuroscience (Oxford)* **2004**, *125*, 867−877.
(28) Frederickson, C. J.; Maret, W.; Cuajungco, M. P. *Neuroscientist* **2004**, *10*, 18−25.
(29) Mocchegiani, E.; Bertoni-Freddari, C.; Marcellini, F.; Malavolta, M. *Prog. Neurobiol.* **2005**, *75*, 367−390.
(30) Bush, A. I. *Trends Neurosci.* **2003**, *26*, 207−214.
(31) Bossy-Wetzel, E.; Talantova, M. V.; Lee, W. D.; Scholzke, M. N.; Harrop, A.; Mathews, E.; Götz, T.; Han, J.; Ellisman, M. H.; Perkins, G. A.; Lipton, S. A. *Neuron* **2004**, *41*, 351−365.
(32) Zhang, Y.; Wang, H.; Li, J.; Jimenez, D. A.; Levitan, E. S.; Aizenman, E.; Rosenberg, P. A. *J. Neurosci.* **2004**, *24*, 10616−10627.
(33) Frederickson, C. J.; Kasarskis, E. J.; Ringo, D.; Frederickson, R. E. *J. Neurosci. Methods* **1987**, *20*, 91−103.
(34) Zalewski, P. D.; Forbes, I. J.; Betts, W. H. *Biochem. J.* **1993**, *296*, 403−408.
(35) Coyle, P.; Zalewski, P. D.; Philcox, J. C.; Forbes, I. J.; Ward, A. D.; Lincoln, S. F.; Mahadevan, I.; Rofe, A. M. *Biochem. J.* **1994**, *303*, 781−786.
(36) Zalewski, P. D.; Forbes, I. J.; Seamark, R. F.; Borlinghaus, R.; Betts, W. H.; Lincoln, S. F.; Ward, A. D. *Chem. Biol.* **1994**, *1*, 153−161.
(37) Takahashi, A.; Camacho, P.; Lechileiter, J. D.; Herman, B. *Physiol. Rev.* **1999**, *79*, 1089−1125.
(38) Kimura, E.; Koike, T. *Chem. Soc. Rev.* **1998**, *27*, 179−184.
(39) Kikuchi, K.; Komatsu, K.; Nagano, T. *Curr. Opin. Chem. Biol.* **2004**, *8*, 182−191.
(40) Jiang, P.; Guo, Z. *Coord. Chem. Rev.* **2004**, *248*, 205−229.
(41) Lim, N. C.; Freake, H. C.; Brückner, C. *Chem. Eur. J.* **2005**, *11*, 38−49.
(42) Hirano, T.; Kikuchi, K.; Urano, Y.; Higuchi, T.; Nagano, T. *Angew. Chem., Int. Ed.* **2000**, *39*, 1052−1054.
(43) Hirano, T.; Kikuchi, K.; Urano, Y.; Nagano, T. *J. Am. Chem. Soc.* **2002**, *124*, 6555−6562.
(44) Komatsu, K.; Kikuchi, K.; Kojima, H.; Urano, Y.; Nagano, T. *J. Am. Chem. Soc.* **2005**, *127*, 10197−10204.
(45) Gee, K. R.; Zhou, Z.-L.; Qian, W.-J.; Kennedy, R. *J. Am. Chem. Soc.* **2002**, *124*, 776−778.
(46) Gee, K. R.; Zhou, Z.-L.; Ton-That, D.; Sensi, S. L.; Weiss, J. H. *Cell Calcium* **2002**, *31*, 245−251.
(47) Burdette, S. C.; Walkup, G. K.; Spingler, B.; Tsien, R. Y.; Lippard, S. J. *J. Am. Chem. Soc.* **2001**, *123*, 7831−7841.
(48) Burdette, S. C.; Frederickson, C. J.; Bu, W.; Lippard, S. J. *J. Am. Chem. Soc.* **2003**, *125*, 1778−1787.
(49) Chang, C. J.; Nolan, E. M.; Jaworski, J.; Burdette, S. C.; Sheng, M.; Lippard, S. J. *Chem. Biol.* **2004**, *11*, 203−210.
(50) Nolan, E. M.; Jaworski, J.; Okamoto, K.-I.; Hayashi, Y.; Sheng, M.; Lippard, S. J. *J. Am. Chem. Soc.* **2005**, *127*, 16812−16823.
(51) Henary, M. M.; Wu, Y.; Fahrni, C. J. *Chem. Eur. J.* **2004**, *10*, 3015−3025.
(52) Woodroofe, C. C.; Lippard, S. J. *J. Am. Chem. Soc.* **2003**, *125*, 11458−11459.
(53) Taki, M.; Wolford, J. L.; O'Halloran, T. V. *J. Am. Chem. Soc.* **2004**, *126*, 712−713.
(54) Chang, C. J.; Jaworski, J.; Nolan, E. M.; Sheng, M.; Lippard, S. J. *Proc. Natl. Acad. Sci. U.S.A.* **2004**, *101*, 1129−1134.
(55) Kiyose, K.; Kojima, H.; Urano, Y.; Nagano, T. *J. Am. Chem. Soc.* **2006**, *128*, 6548−6549.
(56) Thompson, R. B.; Maliwal, B. P. *Anal. Chem.* **1998**, *70*, 1749−1754.
(57) Thompson, R. B.; Whetsell, W. O.; Maliwal, B. P.; Fierke, C. A.; Frederickson, C. J. *J. Neurosci. Methods* **2000**, *96*, 35−45.
(58) Thompson, R. B.; Cramer, M. L.; Bozym, R. *J. Biomed. Opt.* **2002**, *7*, 555−560.
(59) Bozym, R. A.; Thompson, R. B.; Stoddard, A. K.; Fierke, C. A. *ACS Chem. Biol.* **2006**, *1*, 103−111.
(60) Godwin, H. A.; Berg, J. M. *J. Am. Chem. Soc.* **1996**, *118*, 6514−6515.
(61) Walkup, G. K.; Imperiali, B. *J. Am. Chem. Soc.* **1996**, *118*, 3053−3054.
(62) Shults, M. D.; Pearce, D. A.; Imperiali, B. *J. Am. Chem. Soc.* **2003**, *125*, 10591−10597.
(63) Goldsmith, C. R.; Lippard, S. J. *Inorg. Chem.* **2006**, *45*, 555−561.
(64) Nolan, E. M.; Lippard, S. J. *Inorg. Chem.* **2004**, *43*, 8310−8317.

Scheme 1

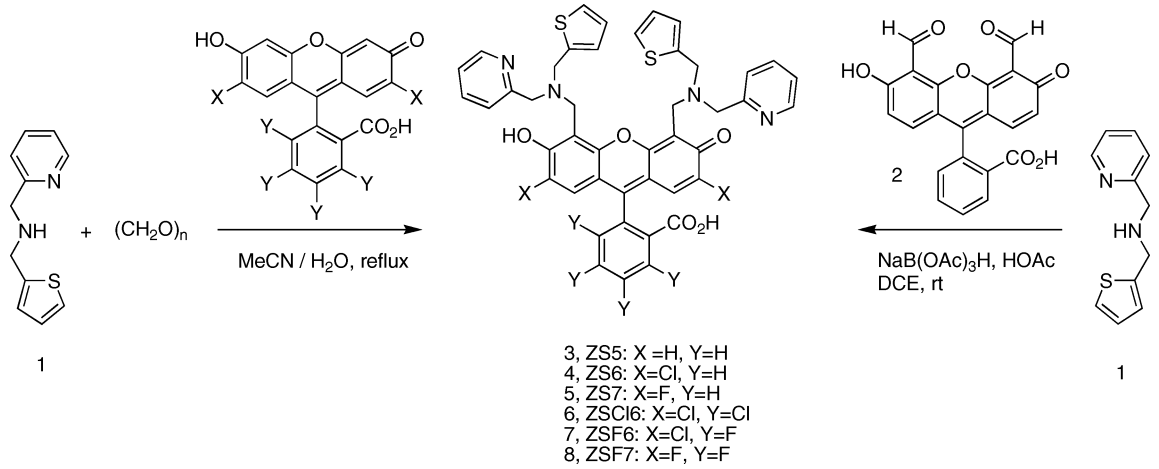

from our laboratory and a recent literature report that indicates groups distant from a fluorophore contribute to PET quenching,[65] we reasoned that incorporating multiple aromatic heterocycles in a tertiary amine-based ligand is important for achieving relatively low background fluorescence and good Zn(II)-induced fluorescence turn-on, at least for symmetrical probes such as ZP1 and ZS1. Substitution of the thioether moiety in ZS1 or ZS2 with a thiophene group is one way to accomplish this task. Moreover, because thiophenes are less basic than pyridyl groups and thioethers, we anticipated that the thiophene moiety would be non-coordinating. The resulting N_2O donor set for Zn(II) binding would confer lower affinity Zn(II) coordination than the N_3O donor sets of the symmetrical ZP systems. In accord with these expectations, the thiophene-for-thioether/pyridine subsitution affords low-micromolar Zn(II) K_d values, improved Zn(II) selectivity, and fluorescence enhancements suitable for biological imaging. We describe extensive confocal microscopic studies of ZS5 (Scheme 1) in cultured cells and in primary cultures of neurons. ZS5 illuminates the mitochondria in HeLa cells, affords a visual image of glutamate-dependent Zn(II) uptake in dendrites of hippocampal neurons, and detects endogenous Zn(II) release in dentate gyrus neurons resulting from nitrosative stress. These findings indicate that ZS5 is a versatile Zn(II) imaging tool with great potential for biological use.

Experimental Section

Reagents. Acetonitrile was dried using columns of aluminum oxide, and anhydrous 1,2-dichloroethane (DCE) was purchased from Aldrich. Methanol was filtered through an aluminum oxide plug before use. Ligand **1**[66] and 4′,5′-fluorescein dicarboxaldehyde (**2**)[47] were prepared as previously described. 2′,7′-Difluorofluorescein was purchased from Invitrogen and 2′,7′-dichlorofluorescein from Aldrich. The latter was recrystallized from boiling EtOH before use. All other halogenated fluorescein derivatives were prepared by acid-catalyzed condensation of the appropriate resorcinol and substituted phthalic anhydride. Additional reagents were obtained from Aldrich and used as received.

Materials and Methods. Merck F254 silica gel plates were used for analytical TLC and were visualized with UV light. Preparative TLC was performed on Whatman silica gel-60 plates of 1 mm thickness, manufactured by EM Science. NMR spectra were acquired on a Varian 300 or 500 MHz spectrophotometer operating at ambient probe temperature, 283 K. The spectra were referenced to internal standards. An Avatar FTIR instrument was used to obtain IR spectra, and the data are included as Supporting Information. High-resolution mass spectra were collected by staff at the MIT Department of Chemistry Instrumentation Facility.

2-{6-Hydroxy-3-oxo-4,5-bis[(pyridin-2-ylmethylthiophen-2-ylmethylamino)methyl]-3*H*-xanthen-9-yl}benzoic Acid (3, Zinspy-5, ZS5). A portion of fluorescein **2** (50 mg, 0.13 mmol) was dissolved in 5 mL of DCE, and 30 μL of HOAc was added. Compound **1** (77 mg, 0.38 mmol) was dissolved in 5 mL of DCE and added to the fluorescein solution in a dropwise manner. The cloudy and orange reaction mixture was stirred for 1 h at room temperature. A portion of $NaB(OAc)_3H$ (70 mg, 0.33 mmol) was added, and the solution clarified. The reaction was stirred overnight at room temperature and became orange-brown. The solution was diluted with 15 mL of $CHCl_3$ and washed with water (3 × 15 mL). The organic portion was dried over $MgSO_4$, and the solvent was removed in vacuo, which gave an orange solid. Preparative TLC on silica gel (20:1 $CHCl_3$/MeOH) gave the product as an orange-red powder (37 mg, 38%); mp > 280 °C, dec. TLC: $R_f = 0.59$ (silica, 9:1 $CHCl_3$/MeOH). ^{1}H NMR (CD_3OD, 300 MHz): δ 3.90 (4H, q), 4.06 (4H, m), 4.15 (4H, m), 6.59 (2H, d), 6.90 (4H, m), 7.05 (2H, m), 7.12 (1H, d), 7.17 (2H, t), 7.25 (2H, d), 7.56 (4H, m), 7.65 (2H, t), 8.00 (1H, d), 8.35 (2H, d). HRMS (ESI): calcd $[M + Na]^+$, 787.2019; found, 787.2024.

2-{2,7-Dichloro-6-hydroxy-3-oxo-4,5-bis[(pyridin-2-ylmethylthiophen-2-ylmethylamino)methyl]-3*H*-xanthen-9-yl}benzoic Acid (4, Zinspy-6, ZS6). Portions of **1** (200 mg, 0.979 mmol) and $(CH_2O)_n$ (50 mg, 1.7 mmol) were combined in 5 mL of MeCN and heated to reflux for 45 min. A slurry of 2′,7′-dichlorofluorescein (131 mg, 0.327 mmol) in 7 mL of 1:1 MeCN/H_2O was added to the reaction, and the solution turned pink. The reaction was heated to reflux for 22 h, during which time a pink precipitate formed, and cooled. The mixture was filtered, and the precipitate was washed with 15 mL of Et_2O. The pure product was obtained as a light pink powder after recrystallization twice from boiling EtOH (223 mg, 85%); mp = 200−201 °C. ^{1}H NMR (DMSO-d_6, 300 MHz): δ 3.96 (8H, m), 4.08 (4H, s), 6.56 (2H, s), 6.96 (4H, m), 7.33−7.43 (8H, m), 7.74−7.87 (5H, m), 7.99 (1H, d), 8.59 (2H, d). HRMS (ESI): calcd $[M - H]^-$, 831.1264; found, 831.1265.

2-{2,7-Difluoro-6-hydroxy-3-oxo-4,5-bis[(pyridin-2-ylmethylthiophen-2-ylmethylamino)methyl]-3*H*-xanthen-9-yl}benzoic Acid (5, Zinspy-7, ZS7). Portions of **1** (83 mg, 0.41 mmol) and $(CH_2O)_n$ (13 mg, 0.45 mmol) were combined in 5 mL of MeCN and heated to reflux for 1 h. A slurry of 2′,7′-difluorofluorescein (50 mg, 0.14 mmol) in 10 mL of 1:1 MeCN/H_2O was added to the reaction, and the solution turned orange. The reaction was heated to reflux for 22 h, and a light

(65) Sparano, B. A.; Shahi, S. P.; Koide, K. *Org. Lett.* **2004**, *6*, 1947−1949.
(66) Banerjee, S. R.; Levadala, M. K.; Lazarova, N.; Wei, L.; Valliant, J. F.; Stephenson, K. A.; Babich, J. W.; Maresca, K. P.; Zubieta, J. *Inorg. Chem.* **2002**, *41*, 6417−6425.

pink precipitate formed. The reaction was cooled to room temperature and filtered, and the precipitate was recrystallized from boiling EtOH twice (71 mg, 60%); mp = 182−183 °C. ^{1}H NMR (DMSO-d_6 with NaOD, 300 MHz): δ 3.74 (4H, s), 3.91 (8H, m), 6.26 (2H, d), 6.88−7.00 (5H, m), 7.13 (2H, m), 7.31 (2H, d), 7.44 (2H, qd), 7.64 (4H, m), 7.98 (1H, dd), 8.36 (2H, d). HRMS (ESI): calcd [M − H]$^-$, 799.1855; found, 799.1866.

2-{2,7-Dichloro-6-hydroxy-3-oxo-4,5-bis[(pyridin-2-ylmethylthiophen-2-ylmethylamino)methyl]-3*H*-xanthen-9-yl}-3,4,5,6-tetrachlorobenzoic Acid (6, Zinspy-Cl6, ZSCl6). Portions of **1** (200 mg, 0.979 mmol) and $(CH_2O)_n$ (48 mg, 1.7 mmol) were combined in 5 mL of MeCN and heated to reflux for 1 h. A slurry of 2′,3,4,5,6,7′-hexachlorofluorescein in 10 mL of 1:1 MeCN/H_2O was added to the reaction, and the solution turned deep magenta. The reaction was heated to reflux for 22 h (during which time a pink precipitate formed), cooled, and filtered. The precipitate was washed with 10 mL of MeCN and recrystallized twice from boiling EtOH, which afforded a light pink powder (255 mg, 80%); mp = 216−217 °C. ^{1}H NMR (DMSO-d_6, 300 MHz): δ 3.95 (8H, s), 4.05 (4H, s), 6.98 (4H, s), 7.26 (2H, s), 7.42 (6H, m), 7.86 (2H, m), 8.63 (2H, m). HRMS (ESI): calcd [M −H]$^-$, 966.9705; found, 966.9705.

2-{2,7-Dichloro-6-hydroxy-3-oxo-4,5-bis[(pyridin-2-ylmethylthiophen-2-ylmethylamino)methyl]-3*H*-xanthen-9-yl}-3,4,5,6-tetrafluorobenzoic Acid (7, Zinspy-F6, ZSF6). Portions of **1** (200 mg, 0.971 mmol) and $(CH_2O)_n$ (48 mg, 1.7 mmol) were combined in 5 mL of MeCN and heated to reflux for 1 h. A slurry of 3,4,5,6-tetrafluoro-2′,7′-dichlorofluorescein in 10 mL of 1:1 MeCN/H_2O was added to the reaction, and the solution turned dark pink. The reaction was refluxed for 22 h, and a pink precipitate formed. The mixture was filtered, and the pink precipitate was washed with 10 mL of H_2O and recrystallized twice from boiling EtOH (208 mg, 68%); mp > 250 °C, dec. ^{1}H NMR (DMSO-d_6, 300 MHz): δ 3.94 (8H, s), 4.04 (4H, s), 6.95 (4H, m), 7.23 (2H, s), 7.41 (6H, m), 7.83 (2H, t), 8.59 (2H, d). HRMS (ESI): calcd [M − H]$^-$, 903.0887; found, 903.0893. Colorless block crystals suitable for X-ray crystallography were grown at room temperature by vapor diffusion of Et_2O into a solution of ZSF6 in CH_2Cl_2.

2-{2,7-Difluoro-6-hydroxy-3-oxo-4,5-bis[(pyridin-2-ylmethylthiophen-2-ylmethylamino)methyl]-3*H*-xanthen-9-yl}-3,4,5,6-tetrafluorobenzoic Acid (8, Zinspy-F7, ZSF7). Portions of **1** (207 mg, 1.01 mmol) and $(CH_2O)_n$ (50 mg, 1.7 mmol) were combined in 6 mL of MeCN and heated to reflux for 30 min. A slurry of 2′,3,4,5,6,7′-hexafluorofluorescein (148 mg, 0.336 mmol) in 10 mL of 1:1 MeCN/H_2O was added to the reaction, and the solution turned deep pink-red. The reaction was heated to reflux for 24 h (during which time a pink precipitate formed), cooled, and filtered. The precipitate was recrystallized twice from boiling EtOH, which gave the product as a pink-orange powder (185 mg, 63%); mp > 250 °C, dec. ^{1}H NMR (DMSO-d_6 with NaOD, 300 MHz): δ 3.78 (4H, s), 3.93 (8H, s), 6.66 (2H, m), 6.89 (4H, m), 7.14 (2H, m), 7.33 (2H, d), 7.51 (2H, m), 7.61 (2H, m), 8.37 (2H, m). HRMS (ESI): calcd [M − H]$^-$, 871.1478; found, 871.1492.

X-ray Crystallographic Studies. Single crystals were mounted on the tips of glass fibers coated with paratone-N oil and cooled to −100 °C under a stream of N_2, maintained by a KRYO-FLEX low-temperature apparatus. Intensity data were collected on a Bruker APEX CCD diffractometer with graphite-monochromated Mo Kα radiation (λ = 0.71073 Å), controlled by a Pentium-based PC running the SMART software package.[67] Data collection and reduction protocols are described elsewhere.[68] Empirical absorption corrections were applied by using the SADABS[69] program, and the structures were solved by direct methods using the SAINTPLUS[70] and SHELXTL[71] software packages. The structures were checked for higher symmetry by using the PLATON software.[72] All non-hydrogen atoms were located and their positions refined with anisotropic thermal parameters by least-squares cycles and Fourier syntheses. Unless otherwise noted, hydrogen atoms were assigned to idealized positions and given thermal parameters equivalent to either 1.5 (methyl hydrogen atoms) or 1.2 (all other hydrogen atoms) times the thermal parameter of the carbon atom to which they were attached.

The structure of ZSF6 contains a dichloromethane molecule that was modeled as disordered over four positions (10:50:15:25). The sulfur and C3 carbon atoms of each thiophene group were modeled as disordered over two positions (50:50). The angles and the 1−2 distances around the sulfur and C3 carbon atoms were constrained to be the same for both components of the disordered thiophene rings. The O1 and O3 hydrogen atoms were located from the electron density map.

General Spectroscopic Methods. Aqueous solutions were prepared with Millipore water. Puratonic grade KCl was purchased from Calbiochem and molecular biology grade piperazine-*N*,*N*′-bis(2-ethanesulfonic acid) (PIPES) from Sigma. With the exception of the pK_a titrations, measurements were generally made at pH 7 in 50 mM PIPES, 100 mM KCl buffer. A buffer containing 50 mM CHES, 100 mM KCl was employed for measurements at pH 9. Parallel experiments in buffer, rigorously treated or not treated with Chelex resin (Bio-Rad, manufacturer protocol) to remove any potentially adventitious metal ions, returned the same dynamic range and K_d values during trials that employed ZS5 or ZS7. Untreated buffer was used for all subsequent experiments. Excess EDTA was added to solutions of apo-ZS prior to quantum yield and extinction coefficient determinations. Zinc stock solutions (100 mM, 500 mM) were prepared from anhydrous 99.999% $ZnCl_2$ (Aldrich) and water. DMSO stock solutions (1 mM) of ZS sensors were prepared, partitioned into ∼300-μL aliquots, stored at 4 or −25 °C, and thawed in the dark before use. A starting solution of 10 mM KOH, 100 mM KCl, pH ∼12, was used for pK_a titrations, and the pH value of the solution was lowered by addition of 6, 2, 1, 0.5, or 0.1 N HCl. Quantum yields were measured by using fluorescein in 0.1 N NaOH (Φ = 0.95) as the standard,[73] as described previously.[47] Excitation was provided at 490 (Zn(II)-bound ZS5 and ZS7), 492 (apo-ZS5), 496 (apo-ZS7 and Zn(II)-bound ZS6), 499 (apo-ZS6), 500 (Zn(II)-bound ZSF7), 503 (apo-ZSF7), 504 (Zn(II)-bound ZSF6), or 505 nm (apo-ZSF6). Extinction coefficients were generally measured over a concentration range of 1−10 μM for the metal-free and Zn(II)-bound species. Apo-ZS5 was an exception, which gives an uncharacteristically low (∼12 000 M^{-1} cm^{-1}) extinction coefficient for symmetrical fluorescein-based sensors such as ZP2[47] and QZ2[50] in the 3−10 μM range under these experimental conditions. Its extinction coefficient was therefore determined over a concentration range of 0−3 μM, which returned an expected value (>30 000 M^{-1} cm^{-1}). For Zn(II) selectivity experiments, ZP1[47] was used as a control for the Fe(II)/Zn(II) studies. Sensors ZS6 and ZSCl6 were not (ZSCl6) or only partially (ZS6) characterized. These probes both suffer from low solubility in most solvents, including DMSO, and poor dynamic range (∼2-fold or less), and thus show little promise for biological imaging applications. Experimental details for all spectroscopic measurements performed in this study are available in the literature.[47,74] All spectroscopic measurements were repeated a minimum of three times using material from at least two separate synthetic preparations, and the resulting averages are reported.

(67) *SMART: Software for the CCD Detector System*, version 5.626; Bruker AXS: Madison, WI, 2000.
(68) Kuzelka, J.; Mukhopadhyay, S.; Spingler, B.; Lippard, S. J. *Inorg. Chem.* **2004**, *43*, 1751−1761.
(69) Sheldrick, G. M. *SADABS: Area-Detector Absorption Correction*; University of Gottingen: Gottingen, Germany, 2001.
(70) *SAINTPLUS: Software for the CCD Detector System*, version 5.01; Bruker AXS: Madison, WI, 1998.
(71) *SHELXTL: Program Library for Structure Solution and Molecular Graphics*, version 6.1; Bruker AXS: Madison, WI, 2001.
(72) Spek, A. L. *PLATON, A Multipurpose Crystallographic Tool*; Utrecht University: Utrecht, The Netherlands, 2000.
(73) Brannon, J. H.; Madge, D. *J. Phys. Chem.* **1978**, *82*, 705−709.
(74) Nolan, E. M.; Burdette, S. C.; Harvey, J. H.; Hilderbrand, S. A.; Lippard, S. J. *Inorg. Chem.* **2004**, *43*, 2624−2635.

Fluorescence spectra were recorded on a Hitachi F-3010 spectrofluorimeter and UV−vis spectra on a Cary IE scanning spectrophotometer, both controlled by manufacturer-supplied software packages. Circulating water baths were used during all acquisitions to maintain the temperature at 25 ± 1 °C. Quartz cells (Starna) with a 1-cm path length were used for all measurements.

Dissociation Constant Determination. The apparent zinc complex dissociation constants for select ZS probes were determined by fluorimetric analysis. In a typical experiment, a 1 μM solution of the ZS compound was prepared (50 mM PIPES, 100 mM KCl, pH 7) and its emission spectrum recorded. Various aliquots of 1 or 10 mM aqueous $ZnCl_2$ solutions were added, and the emission change was noted. The data were integrated, normalized with respect to the full response, and plotted against the total concentration of Zn(II) in solution. The data were fit to a 1:1 metal−ligand binding model.[75]

Stopped-Flow Kinetic Studies. Single-mixing stopped-flow kinetics studies were performed with a Hi-Tech SF-61 DX2 double-mixing stopped-flow apparatus equipped with a fluorescence detector. Excitation was provided at 490 (ZS5, ZS7), 505 (ZS6), 510 (ZSF7), or 520 nm (ZSF6). A GG495 glass cutoff filter (<455 nm) was placed over the exit of the photomultiplier tube, and the emission was monitored from 455 to 700 nm. All solutions were prepared in 50 mM PIPES, 100 mM KCl, pH 7 buffer. Conditions for pseudo-first-order kinetics were maintained by using at least a 10-fold excess of Zn(II) in all experiments. Except for temperature-dependent studies, all experiments were conducted at 4.3 ± 0.1 °C. The temperature inside the sample chamber was monitored with an internal thermocouple. A series of control experiments were conducted in which the initial ZS concentration was varied from 0.5 to 5 μM after mixing to ensure that the observed rate constant was independent of initial dye concentration (data not shown). Multiple shots were taken for each Zn(II) (or sensor) concentration and averaged. Experiments were conducted three times with fresh Zn(II), sensor, and buffer solutions, and the resulting averages and standard deviations are reported. Observed rate constants were obtained by fitting individual traces to monoexponentials. The KinetAssyst software package (HiTech) was used to analyze the data. Further experimental details are available elsewhere.[50]

Cell Culture. HeLa, COS-7, and HEK293-T cells were cultured in Dulbecco's Modified Eagle Medium (DMEM, Invitrogen) supplemented with 10% fetal calf serum (FCS, Invitrogen), glutamine (2 mM), penicillin (100 units/mL), and streptomycin (100 μg/mL). Two days before imaging, the cells were passed and plated on untreated (HeLa, COS-7) 10-mm glass coverslips or on glass coverslips coated with 0.2% gelatin for at least 1 h at room temperature (HEK293-T). For labeling, the growth medium was removed and replaced with DMEM containing 1% FCS. The cells were treated and incubated with 10 μM sensor at 37 °C under 5% CO_2 for 30 min. The cells were washed once with and bathed in DMEM containing no FCS prior to imaging and/or zinc addition. Zinc was introduced to the cultured cells as the pyrithione salt using a Zn(II)/pyrithione ratio of 1:1 or 1:2. Stock solutions of $ZnCl_2$ (10 mM) and sodium pyrithione (20 mM) in DMSO were combined and diluted 10-fold with DMEM prior to addition. In a typical experiment, a 100-μL aliquot of this solution was added to the cells bathed in 2 mL of DMEM. A stock solution of TPEN (10 or 20 mM) was also diluted 10-fold with DMEM containing no FCS prior to cell treatment. *S*-Nitrosocysteine (SNOC, 10 mM) was prepared immediately before use according to a literature procedure.[76]

Lysotracker Red (Invitrogen) and Mitotracker Red (Invitrogen) were employed for co-localization studies. In a typical experiment, a 1 mM solution of either marker in DMSO was diluted 100- to 200-fold with DMEM prior to cell treatment. The exact concentration of Lysotracker or Mitotracker used varied with lot number and was in the range of 100−500 nM. The cells were co-treated with the organelle marker and ZS5 or ZP3 and were generally incubated with the reagents for 30 min (37 °C, 5% CO_2) before imaging.

A pGolgi-DsRed construct was employed to label the Golgi apparatus. This plasmid expresses a fusion protein consisting of DsRed and a sequence encoding the N-terminal 81 amino acids of human β-1,4-galactosyltransferase (Clonetech). The latter sequence includes a membrane-anchoring signal peptide, which directs the fusion protein to the trans-Golgi region. Overexpression of pGolgi-DsRed results in its presence in other compartments of the secretory pathway. HeLa cells were passed and plated onto untreated 10-mm glass coverslips 36 h before transfection. The cells were transiently transfected with pGolgi-DsRed using the Lipofectamine reagent (manufacturer protocol) 24−36 h prior to imaging.

Preparation of Embryonic Hippocampal Neuronal Cultures. Hippocampal primary cultures were prepared from day 19 (E19) Sprague−Dawley rat embryos according to a previously reported protocol.[77] Medium-density cultures (150 cells/mm^2) were plated on 24-mm glass coverslips coated with poly-D-lysine (30 μg/mL) and laminin (2.5 μg/mL). Hippocampal cultures were grown in Neurobasal media (Invitrogen) supplemented with B27 (Invitrogen), glutamine (0.5 mM), and glutamate (12.5 μM). After 16−20 days in culture, the medium was removed and replaced with fresh Neurobasal containing no B27. The cells were stained by bath application of the appropriate dye to the media and incubated at 37 °C under 5% CO_2. The ZS5 stock solution (1 mM in DMSO) was diluted 10-fold with either Neurobasal or PBS before addition. The Zn(II)/pyrithione mix has poor solubility in Neurobasal, so these DMSO stock solutions were diluted with either PBS or serum-free DMEM before addition. In some instances, the neurons were transfected with 3.6 μg of β-actin dsRed DNA using Lipofectamine 2000 (manufacturer protocol). The neurons were incubated with the DNA/lipofectamine mix for 1 h (37 °C, 5% CO_2) on DIV 16, washed with and bathed in the growth medium, and imaged on DIV 19 or 20. Solutions of Zn(II)/glutamate (1:2 Zn(II)/glutamate ratio) were prepared in PBS from aqueous solutions of $ZnCl_2$ (10 mM) and glutamate (10 mM) and used immediately. Experiments were conducted in a minimum of four independently prepared cultures.

Preparation of Postnatal Dentate Gyrus Neuronal Cultures. Primary cultures of dentate gyrus (DG) cells were prepared by modification of a literature procedure.[78] DG regions were dissected from the hippocampi of 4-day-old Sprague Dawley rat pups. The cells were plated on 24-mm glass coverslips (250 cells/mm^3) coated with poly-L-lysine (Sigma, 50 μg/mL). The cultures were maintained for the first 24 h in DMEM (Invitrogen) supplemented with 10% FCS (Invitrogen), glutamine (2 mM), and penicillin−streptomycin mix (50 μg/mL). Subsequently, the cells were kept in Neurobasal medium (Invitrogen) supplemented with B27 (Invitrogen), glutamine (2 mM), potassium chloride (20 mM), and penicillin−streptomycin mix (50 μg/mL). After 7 days in culture, the medium was removed and replaced with Neurobasal containing no B27, and the cells were treated with ZS5 and Zn(II)/pyrithione as described above for the hippocampal neurons. For experiments requiring SNOC, the reagent was prepared immediately before use and added to the cells by application on the microscope stage. Experiments were conducted with two independently prepared cultures.

Cytotoxicity Assays in HeLa Cells. To ascertain the cytotoxic effect of sensor treatment over a 24-h period, HeLa cells were passed and plated to ~60% confluence in 12-well plates 12−16 h before treatment and bathed in 1 mL of DMEM supplemented as described above. Prior to ZP treatment, the DMEM was removed and replaced with fresh DMEM, and aliquots of ZP1,[47] ZP3,[49] or ZS5 stock solutions (1 mM DMSO) were added for final concentrations of 1, 5, and 10 μM. The treated cells were incubated for 24 h at 37 °C and under 5% CO_2. Subsequently, the cells were treated with 5 mg/mL MTT (100 μL/

(75) Lim, M. H.; Xu, D.; Lippard, S. J. *Nat. Chem. Biol.* **2006**, *2*, 375−380.
(76) Kröncke, K.-D.; Kolb-Bachofen, V. *Methods Enzymol.* **1999**, *301*, 126−135.
(77) Brewer, G. J.; Toricelli, J. R.; Evege, E. K.; Price, P. J. *J. Neurosci. Res.* **1993**, *35*, 567−576.
(78) Figiel, I.; Kaczmarek, L. *Neurochem. Int.* **1997**, *31*, 299−240.

well) and incubated for an additional 2−4 h (37 °C, 5% CO_2). The DMEM was removed, the cells were dissolved in DMSO (500 μL/well), and the absorbance at 550 nm was recorded. Three independent trials were conducted, and the averages and standard deviations are reported. The reported percent cell survival values are relative to untreated control cells. Additional control studies indicated that the DMSO added (1−10 μL) as a result of sensor treatment has no effect on cell viability under these conditions. The HeLa cells used were at P-10 to P-16, and the assays were repeated using a minimum of two separate HeLa cell stocks.

Laser Scanning Confocal Microscopy. A Zeiss LSM510 microscope equipped with a 63× or 100× oil-immersion objective was used to obtain confocal images. For co-localization experiments, electronic zoom (1.5×) was used in combination with the 100× objective. Samples were excited at 488 nm with an Ar laser. The microscope stage was outfitted with a CTI-3700 incubator, which maintained samples at 37 °C and under 5% CO_2. With the exception of ZS5 treatment, which was performed in a tissue culture hood, addition of all reagents was carried out by bath application on the microscope stage.

Results and Discussion

Design and Syntheses of Probes. Two main considerations influenced the design of the sensors described in this work. Our primary goal was to improve the dynamic range and maintain both the Zn(II) selectivity and relatively low Zn(II) affinity of thioether-containing ZS sensors. We therefore substituted the thioether moiety of our first-generation ZS sensors with a thiophene group. We anticipated that replacement of an alkyl chain with an aromatic heterocycle would result in lower background emission and, in turn, greater fluorescence enhancement following Zn(II) coordination. A second objective was to prepare sensors in relatively few steps and high yield. For this reason, we focus on symmetrical species with tertiary-amine-based ligands, which can generally be obtained in six or fewer steps from commercially available materials.

Scheme 1 illustrates the syntheses of symmetrical ZS sensors **3**−**8** from fluorescein precursors. Probes containing halogenated fluorophores were prepared by Mannich reactions of the fluorescein and the imminium ion condensation product of paraformaldehyde and **1**. In each case, the desired product precipitated from the reaction solution, and multiple (two or three) recrystallizations of the precipitates from boiling EtOH yielded sensors **4**−**8** as light to bright pink powders in moderate to high yields. Fluorescein-based ZS5 (**3**) was prepared from **1** and dialdehyde **2** (Scheme 1) using $NaB(OAc)_3H$ as the reducing agent and obtained in moderate yield after workup and preparative TLC on silica gel

There are few reported crystal structures of fluorescein-based compounds. This paucity most likely stems from the fact that fluoresceins can adopt many isomers, including quinoid and lactone forms, which makes crystallization difficult. Since we could easily prepare relatively large (often >100 mg) quantities of the ZS sensors described in this work, we were able, through multiple attempts, to obtain X-ray-quality crystals of a ZS sensor. Single crystals of ZSF6 were obtained by vapor diffusion of Et_2O into a solution of the sensor in CH_2Cl_2 at room temperature. Figure 2 displays the ORTEP diagram of ZSF6, and Tables S1 and S2 (Supporting Information) provide crystallographic parameters and selected bond lengths and angles, respectively. ZSF6 crystallized in the lactone form, affording a colorless and non-fluorescent material, as previously

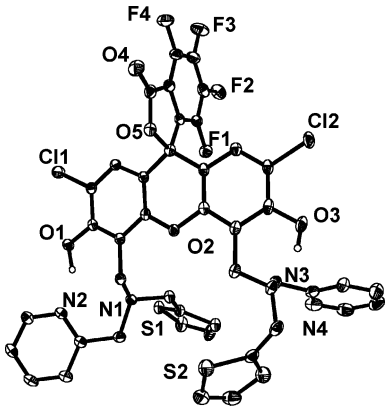

Figure 2. ORTEP diagram for the structure of ZSF6, showing 40% probability ellipsoids on all non-hydrogen atoms.

observed for the dinuclear ZP1:Zn(II) complex[47] and ZPCl1.[79] The hydrogen atoms of O1 and O3 were located from a difference electron density map, and both form hydrogen bonds with the nitrogen atoms of the pyridyl−amine−thiophene moieties. The O1 proton is hydrogen-bonded to both the tertiary amine N1 and pyridyl N2 atoms, with O1−N1 and O1−N2 distances of 3.190(3) and 2.599(3) Å, respectively. The O3 proton is hydrogen-bonded to the tertiary amine N3 atom, with an O3−N3 distance of 2.634(3) Å. No hydrogen-bonding interactions are observed with the thiophene moieties, as expected given the poor basicity of this group.

Photophysical Properties of Thiophene-Containing ZS Sensors. Table 1 summarizes photophysical characterization and thermodynamic parameters for ZS sensors, in addition to data for the symmetrical ZP probes for comparison. In general, halogenation of the fluorescein platform induces red-shifts in both excitation and emission maxima. Chlorination or fluorination of the benzoate rings causes ca. 20 nm red-shifts, and chlorination of the 2′ and 7′ positions of the xanthenone framework also results in red-shifts relative to fluorescein and its 2′,7′-difluoro derivative. These substitutions afford an excitation and emission range of ∼35 nm, similar to that of the halogenated ZP family.[49] Although modest, this feature could be useful for biological imaging experiments that require two Zn(II)-specific probes or for dual Zn(II) and Ca(II) sensing.

Introduction of a thiophene group into the metal-binding unit results in lower background emission and greater fluorescence enhancement than observed for thioether-containing ZS1 and ZS2. This trend is particularly evident for the ZS2/ZS7 pair, where Φ_{free} decreases from 0.39 to 0.25 (50 mM PIPES, 100 mM KCl, pH 7). As a result, the quantum yields and dynamic ranges of thiophene-containing ZS more closely resemble those of the ZP family, although Φ_{free} is consistently higher and indicates that DPA quenches the fluorescein excited state more effectively than the pyridyl−amine−thiophene moiety. Depending on the substitution pattern on the fluorescein rings, compounds **3**−**8** offer ∼2- (ZS6, ZSCl6) to >4.5-fold (ZSF7) fluorescence turn-on following Zn(II) coordination. Representative emission spectra are given in Figures 3 and S1−S3 (Supporting Information). The optical absorption spectra of both Zn(II)-free and -bound forms of the ZS sensors are characterized by high molar extinction coefficients, and Zn(II) coordination results in a slight (ca. 10 nm) blue-shift and increase in the molar

(79) Nolan, E. M.; Lippard, S. J. Unpublished results.

Table 1. Spectroscopic and Thermodynamic Data for Symmetrical ZP and ZS Sensors[a]

	absorption λ_{max} (nm), $\epsilon_{max} \times 10^4$ (M^{-1} cm^{-1})		emission λ_{max} (nm), Φ[b]				
	unbound	Zn(II)	unbound	Zn(II)	pK_{a1} (N)[c]	pK_{a2}[d]	ref
ZP1	515, 7.9	507, 8.4	531, 0.38	527, 0.87	8.4	2.8	47
ZP2	498, 4.4	490, 5.3	522, 0.25	517, 0.92	9.4	3.9	47
ZP3	502, 7.5	492, 8.5	521, 0.15	516, 0.92	6.8	2.0	49
ZPF1	533, 9.9	525, 12.0	547, 0.11	544, 0.55	6.9	1.8	49
ZPCl1	534, 9.7	527, 12.0	550, 0.22	549, 0.50	7.0	1.9	49
ZPF3	520, 8.7	510, 9.3	537, 0.14	533, 0.60	6.7	1.9	49
ZS1	510, 8.4	501, 7.5	531, 0.50	526, 0.70	7.7	2.0	64
ZS2	499, 6.7	489, 6.8	523, 0.39	516, 0.69	7.7	2.7	64
ZS5	497, 3.3	490, 4.2	522, 0.36	517, 0.80	8.0	4.6	this work
ZS6	515, n.d.	505, n.d.	533, 0.44	527, 0.64	7.8	3.3	this work
ZSF6	532, 6.3	522, 7.0	549, 0.19	545, 0.63	7.1	2.0	this work
ZS7	500, 6.2	490, 6.6	524, 0.25	518, 0.79	7.0	2.7	this work
ZSF7	521, 6.2	511, 7.0	535, 0.24	527, 0.68	6.9	2.5	this work

[a] All quantum yield and extinction coefficient measurements were conducted at pH 7 (50 mM PIPES, 100 mM KCl). [b] Quantum yields were measured using fluorescein in 0.1 N NaOH as a standard (Φ = 0.95, ref 73). [c] The pK_a value associated with fluorescence enhancement as the pH is lowered. This pK_a is assigned to tertiary amine protonation. [d] The pK_a value associated with fluorescence quenching as the pH is lowered.

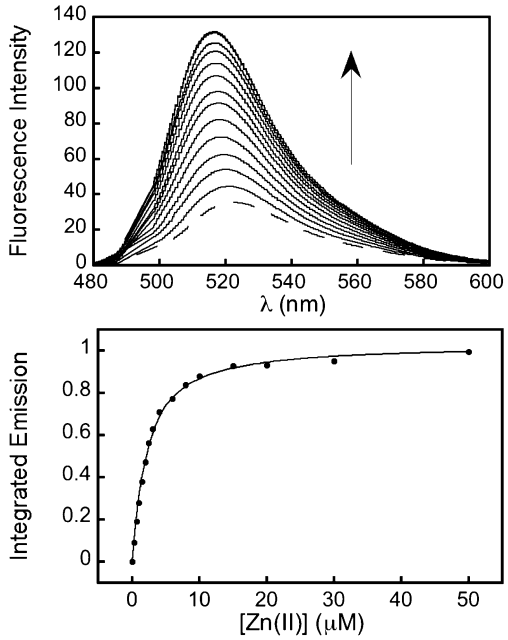

Figure 3. Fluorescence response of 1 μM ZS5 to Zn(II). Top: Response of ZS5 to Zn(II) at pH 7 (50 mM PIPES, 100 mM KCl) and 25 °C. Bottom: Integrated emission vs Zn(II) concentration for ZS5. Aliquots of 1 and 10 mM $ZnCl_2$ were added to afford 0, 0.33, 0.66, 1, 1.5, 2.0, 2.5, 3.0, 4.0, 6.0, 8.0, 10, 15, 20, 30, and 50 μM Zn(II). The circles depict the experimental data, and the line is the fit to a 1:1 metal−ligand binding model. Excitation was provided at 490 nm.

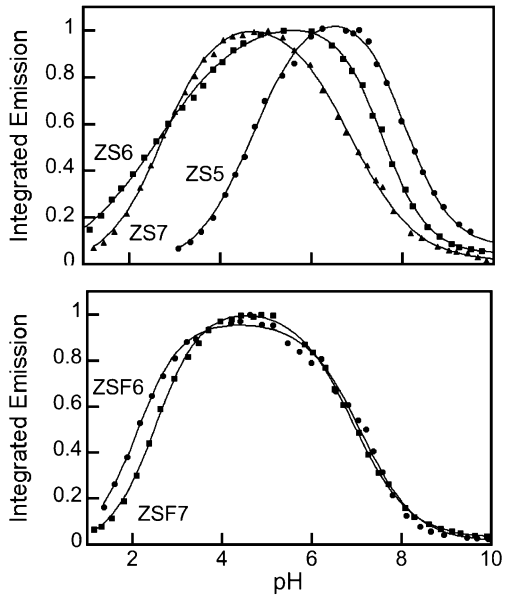

Figure 4. Effect of pH on integrated emission (100 mM KCl, 25 °C). Top plot: Representative pH titrations for ZS5 (circles), ZS6 (squares), and ZS7 (diamonds). Bottom plot: Representative pH titrations for ZSF6 (circles) and ZSF7 (squares). For each titration, a 1 μM solution of ZS was prepared (10 mM KOH, 100 mM KCl, pH ~12), and the pH was lowered by incremental addition of aqueous HCl. Data for pH >12 are excluded from the plots, since no appreciable fluorescence change occurred in this range. The pK_a values, obtained from fitting the experimental data to a nonlinear model,[47] are listed in Table 1.

absorptivity. This behavior parallels that of many previously characterized ZS and ZP sensors and indicates that the phenol moiety is involved in Zn(II) coordination.

The data in Table 1 reveal that substitution of the 2′ and 7′ positions of the xanthenone moiety causes systematic variations in Φ_{free} that are independent of ligand type. For both ZP and ZS, the magnitude of Φ_{free} decreases as X = Cl > H > F. Similar background fluorescence reduction has been observed by others upon substitution of fluorescein with 2′,7′-difluorofluorescein.[43] Although the origin of this effect is unclear, it is generally applicable to the design of fluorescein-based metal ion sensors.

The ZS sensors presented in this study operate via a PET mechanism.[80] Sensors of this type are often pH-sensitive. Figure 4 displays representative pH titrations for selected probes, and pK_a values are given in Table 1. We first consider ZS5−7, which lack benzoate ring halogenation (Figure 4, top). Like ZP1−3, the 2′,7′-dichloro (ZS6) and 2′,7′-difluoro platforms (ZS7) shift the pH titration curve toward lower values relative to that of the unsubstituted fluroescein (ZS5). This trend parallels the known pH-dependent emission profiles and pK_a values of the parent fluorophores, with fluorescein having a phenolic pK_a value of 6.4,[81] compared to 5.0[82] for 2′,7′-dichloro- and 4.8[83]

(80) de Silva, A. P.; Gunaratne, H. Q. N.; Gunnlaugsson, T.; Huxley, A. J. M.; McCoy, C. P.; Rademacher, J. T.; Rice, T. E. *Chem. Rev.* **1997**, *97*, 1515−1566.
(81) Sjöback, R.; Nygren, J.; Kubista, M. *Spectrochim. Acta Part A* **1995**, *51*, L7−L21.
(82) Leonhardt, H.; Gordon, L.; Livingston, R. *J. Phys. Chem.* **1971**, *75*, 245−249.
(83) Sun, W.-C.; Gee, K. R.; Klaubert, D. H.; Haugland, R. P. *J. Org. Chem.* **1997**, *62*, 6469−6475.

Table 2. Kinetic and Thermodynamic Parameters for Zn(II) Binding to Selected Sensors[a]

	k_{on} (M^{-1} s^{-1})[b] 4.3 °C	k_{on} (M^{-1} s^{-1})[c] 25 °C	K_{d1}[d] 25 °C	k_{off} (s^{-1})[e] 25 °C	$\Delta H^{\ddagger}$ (kcal/mol)[f]	$\Delta S^{\ddagger}$ (cal/mol·K)[f]
ZP1	$(6.3 \pm 0.1) \times 10^5$	$(3.3 \pm 0.4) \times 10^6$	0.7 ± 0.1 nM	$(2.3 \pm 0.4) \times 10^{-3}$	12.5 ± 0.1	13.2 ± 0.3
ZP3	$(7.8 \pm 0.1) \times 10^5$	$(4.3 \pm 0.3) \times 10^6$	0.7 ± 0.1 nM	$(2.9 \pm 0.4) \times 10^{-3}$	11.6 ± 0.2	10.7 ± 0.7
ZS5	$(3.6 \pm 0.2) \times 10^5$	$(2.2 \pm 0.1) \times 10^6$	1.5 ± 0.2 μM	3.3	13.3 ± 0.1	15.2 ± 0.2
ZS6	$(3.7 \pm 0.1) \times 10^5$	$(2.1 \pm 0.1) \times 10^6$	n.d.	n.d.	12.9 ± 0.4	14.0 ± 0.7
ZS7	$(5.9 \pm 0.1) \times 10^5$	$(3.0 \pm 0.1) \times 10^6$	3.7 ± 0.2 μM	11	12.5 ± 0.3	12.9 ± 1.3
ZSF6	$(3.3 \pm 0.1) \times 10^5$	$(1.8 \pm 0.1) \times 10^6$	4.6 ± 0.2 μM	8.3	12.6 ± 0.2	12.4 ± 0.9
ZSF7	$(5.0 \pm 0.1) \times 10^5$	$(2.7 \pm 0.1) \times 10^6$	5.0 ± 0.3 μM	13.5	12.6 ± 0.2	13.0 ± 0.7

[a] All measurements were made at pH 7 (50 mM PIPES, 100 mM KCl). Data for ZP1 and ZP3 are taken from ref 50. [b] Experimentally determined values for k_{on} at 4.3 ± 0.1 °C. [c] Experimentally determined values for k_{on} at 25 ± 0.1 °C. [d] Dissociation constants obtained experimentally by fluorimetric titration at 25 ± 1 °C. [e] Calculated k_{off} for ZS at 25 °C. [f] Activation parameters were determined over a temperature range of ~4 to ~40 °C.

for 2′,7′-difluorofluorescein. As a result, the pK_a transition assigned to tertiary amine protonation decreases from 8.0 (ZS5, X = H) to 7.0 (ZS7, X = F). Fluorescence quenching occurs at pH <~6 when the phenol group becomes protonated. These pK_a values range from 4.6 to 2.7 with X = H > Cl ~ F.

Titrations of bottom-ring-halogenated ZSF6 and ZSF7 are given in the bottom panel of Figure 4. These profiles are both characterized by two pK_a transitions, with p$K_{a1} \approx 7$ assigned to tertiary amine protonation and p$K_{a2} < 3$ assigned to protonation of the phenol. The pK_{a1} values are similar to those observed for ZPF1 (p$K_a = 6.9$) and ZPF3 (p$K_a = 6.7$) and follow the same trend of further diminution upon fluorination of the 2′ and 7′ positions. Scheme S1 depicts the protonation equibria for the thiophene-containing ZS sensors proposed on the basis of these experiments and on the low basicity of thiophene moieties.

The titrations in Figure 4 illustrate that emission of the ZS sensors is effectively quenched at high pH. The quantum yield of apo-ZS5 drops from 0.36 at pH 7 to 0.04 at pH 9. As a result, ZS5 shows >20-fold fluorescence enhancement following Zn(II) coordination at pH 9, with $\Phi_{Zn} = 0.73$ (50 mM CHES, 100 mM KCl), as compared to ~4-fold enhancement at pH 7 (50 mM PIPES, 100 mM KCl). This behavior is consistent with the PET mechanism.

Metal-Binding Properties. I. Zinc Affinity and Coordination. Fluorescence spectroscopy was used to determine apparent Zn(II) complex K_d values for ZS5, ZSF6, ZS7, and ZSF7, which are listed in Table 2. Representative binding curves are given in Figure 3 (ZS5) and as Supporting Information (ZSF6, ZS7, ZSF7). Fluorescein-based ZS5 exhibits maximum fluorescence in the presence of ~10 equiv of Zn(II) and has a K_d value of 1.5 ± 0.2 μM. This value is ~3 orders of magnitude greater than the K_{d1} value of ZP2 ($K_{d1} = 0.5 \pm 0.1$ nM)[47] and about twice that of asymmetrical ZP9 ($K_d = 0.69 \pm 0.04$ μM).[84]

Halogenation of the xanthenone and benzoate moieties raises the K_d significantly, with values for ZS7, ZSF6, and ZSF7 of 3.7 ± 0.4, 4.6 ± 0.2, and 5.0 ± 0.3 μM, respectively. We attribute this behavior to variation in the donor ability of the deprotonated phenol group. Incorporation of halogens reduces the electron density on the oxygen atom, making it a poor donor relative to X = H. As a result, the Zn−O bond is weaker in chlorinated and fluorinated ZS relative to ZS5. This trend is in accord with the pH studies on fluorescein and its halogenated derivatives, where the pK_a of the phenol decreases with chlorination and fluorination of the fluorescein platform, respectively.[82,83] This behavior is somewhat evident in the K_d values for the symmetrical ZP probes, which range from 0.5 to 1.1 nM.[49]

Thiophenes are weak bases with low affinity for many divalent metal ions, including Zn(II). To establish that the thiophene moiety is not involved in Zn(II) coordination, X-ray crystallographic studies were conducted using a salicylaldehyde-based model of ZS5. A report of this study is given as Supporting Information. Single crystals were obtained from small-scale crystallization trials, and X-ray structural determination of these complexes confirmed that the thiophene moiety of the model ligand does not bind to Zn(II) or to other divalent first-row transition metal ions, including Cu(II) (Figure S4).

Sensors **3**−**8** have two possible metal-binding sites. By analogy to the symmetrical ZP systems and from chemical intuition, we propose stepwise binding with formation of the 1:1 ZS:Zn(II) complexes at relatively low Zn(II) concentrations and formation of 1:2 complexes at significantly higher concentrations of Zn(II). Fluorimetric titrations show that the fluorescence response of 1 μM ZS to Zn(II) maximizes at 10−50 μM Zn(II), depending on the fluorophore platform, which indicates that the second binding event has little influence on the fluorescence response. For this reason, values for K_{d2} were not determined.

II. Zinc Selectivity. One objective of this investigation was to maintain the Zn(II) selectivity observed for thioether-containing ZS. Figure 5 illustrates the selectivity of ZS5 for Zn(II) in the presence of biologically relevant cations, divalent first-row transition metal ions, Cd(II) and Hg(II). The data for the halogenated sensors are generally analogous, although the degree of quenching observed following Hg(II) addition varies with fluorescein halogenation. As anticipated, the behavior of ZS5 follows that of ZS1−4, maintaining the selectivity for Zn(II) over Fe(II). The greater affinity of ZS5 for Zn(II) vs Hg(II) is an improvement over the thioether-containing ZS sensors because Zn(II) addition to solutions of ZS1−4 and Hg(II) does not cause any fluorescence change.[64] This difference results from loss of a strong Hg−S bond between the metal ion center and the thioether donor.

III. Kinetics and Thermodynamics of Zn(II) Association. The fluorescence responses of the ZS probes are observable immediately after Zn(II) addition. We therefore conducted stopped-flow kinetic studies to determine the rate constants for Zn(II) association, measured by fluorescence turn-on, for these sensors. Table 2 lists the experimentally determined second-order rate constants for Zn(II) association (k_{on}) and, in most instances, calculated rate constants for Zn(II) dissociation (k_{off}).

(84) Nolan, E. M.; Jaworski, J.; Racine, M. E.; Sheng, M.; Lippard, S. J. *Inorg. Chem.*, published ASAP online October 31, 2006, http://dx.doi.org/10.1021/ic061137c.

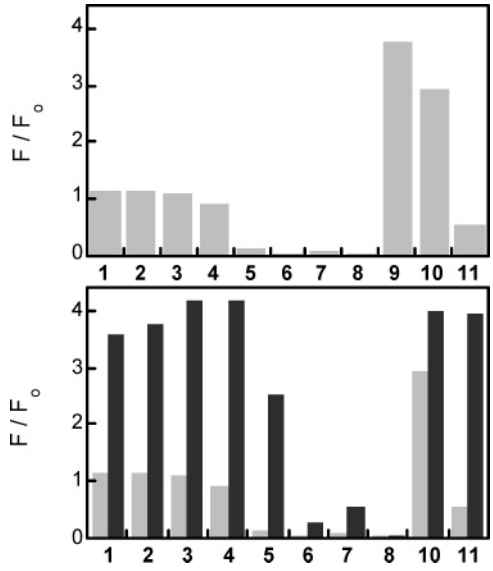

Figure 5. Selectivity of ZS5 for Zn(II) at pH 7 (50 mM PIPES, 100 mM KCl). Top plot: Fluorescence response of 1 μM ZS5 to 50 equiv of the cation of interest: 1, Na(I); 2, Ca(II); 3, Mg(II); 4, Mn(II); 5, Fe(II); 6, Co(II); 7, Ni(II); 8, Cu(II); 9, Zn(II); 10, Cd(II); 11, Hg(II). Bottom plot: The light gray bars correspond to the bars in the top plot. The black bars illustrate the fluorescence change that occurs immediately after 50 equiv of Zn(II) is added to the solution containing 1 μM ZS5 and 50 equiv of the cation of interest. All data (F) are normalized with respect to the emission from the free sensor (F_o). Excitation was provided at 490 nm and 25 °C.

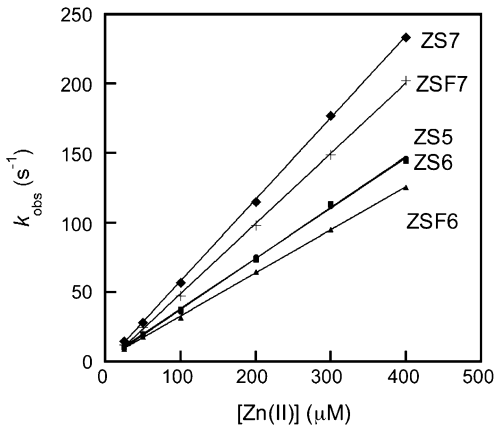

Figure 6. Plots of k_{obs} vs Zn(II) concentration for ZS family members obtained from stopped-flow fluorescence studies at pH 7 (50 mM PIPES, 100 mM KCl) and 4.3 °C. The concentration of ZS was 0.5 μM after mixing, and the concentration of Zn(II) was varied from 0 to 400 μM after mixing. Experimentally determined Zn(II) association (k_{on}) and calculated Zn(II) dissociation (k_{off}) rate constants are given in Table 2.

Plots of k_{obs} versus Zn(II) concentration are given in Figure 6, which return k_{on} values ranging from 3.3×10^5 to 5.9×10^5 M^{-1} s^{-1} at 4.3 °C. Data from temperature variation experiments indicate k_{on} values of 1.8×10^6 to 3.0×10^6 M^{-1} s^{-1} at 25 °C, which are comparable to those of DPA-based probes such as ZP[50] and ZnAF[44] family members. The dissociation rate constants, k_{off}, were calculated from the experimentally determined k_{on} and K_d values and range from 3.3 to 13.5 s^{-1} at 25 °C, yielding $t_{1/2}$ values of 50−210 ms. These kinetic parameters demonstrate that the ZS sensors bind Zn(II) both rapidly and, significantly, more reversibly than DPA-based ZP. Furthermore, these data are in accord with rate constants obtained for ZnAF probes, which indicated that (i) one pyridyl group in a DPA-like chelate is sufficient for maintaining fast Zn(II) complexation and (ii) the rate of Zn(II) dissociation is significantly more sensitive to loss of a DPA pyridyl group.[44]

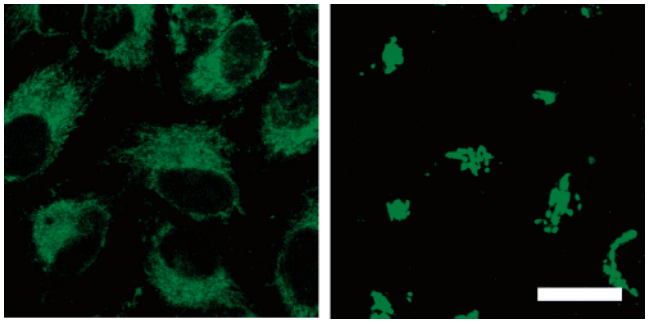

Figure 7. Comparison of subcellular compartmentalization of ZS5 (left) and ZP3 (right) in HeLa cells. Both confocal images were obtained 5 min after addition of 100 μM Zn(II)/pyrithione to cells treated with 10 μM ZS5 or ZP3 (37 °C, 5% CO_2). Addition of Zn(II)/pyrithione has no effect on sensor localization during this time frame. The scale bar is 25 μm.

Halogenation of the fluorescein platform has subtle effects on the k_{on} values. Both the ZP1/ZP3 and ZS6/ZS7 couples show that fluorination of the 2′ and 7′ positions increases the magnitude of k_{on} relative to chlorination. Comparison of the ZS couples ZS6/ZSF6 and ZS7/ZSF7 indicates that fluorination of the benzoate moiety decreases k_{on} to some degree.

Temperature variation experiments were conducted to determine the activation enthalpies and entropies for Zn(II) coordination to the ZS sensors, and these data are also included in Table 2. Figure S6 displays representative Eyring plots for each probe, from which we compute $\Delta H^{\ddagger}$ to be 12.6−13.3 kcal/mol and $\Delta S^{\ddagger}$ to range from 12.4 to 15.2 cal/mol·K. The former values are indicative of a low activation barrier and fast association rate; they are comparable to those determined for ZP family members. The positive $\Delta S^{\ddagger}$ values are also typical of fluorescein-based sensors designed in our laboratory, which we presume reflect loss of water molecules or buffer components from the Zn(II) center or loss of protons from ZS in the transition state during binding.

Biological Imaging Studies. I. Response of ZS5 to Zinc in Cultured Cells and Subcellular Localization. Several features of the ZS probes, including improved dynamic range relative to the thioether-containing parent compounds and low-micromolar affinity for Zn(II), motivated us to consider their utility for in vivo work. We began these investigations with ZS5, the first compound we prepared, and quickly found that it is amenable for such experiments. We therefore focused our attention on this probe for biological imaging.

Initial cell studies indicated that ZS5 permeates a number of commercially available immortal cell lines and is Zn(II)-responsive in vivo. Figure S7 exhibits representative images of ZS5-treated HeLa, COS-7, and HEK293-T cells. In preliminary work, the cells were treated with 10 μM ZS5 for varying incubation times, which reveal 30 min (37 °C, 5% CO_2) to be optimal. Longer incubation periods (>1 h) are also acceptable, but shorter (ca. 20 min or less) ones result in insufficient sensor uptake. Addition of Zn(II) to the cells as the 1:1 or 1:2 Zn(II)/pyrithione complex affords intracellular fluorescence enhancement, which is reversed with TPEN treatment (Figure S7).

An important observation from these preliminary experiments concerned the subcellular localization of ZS5 in HeLa cells. Figure 7 shows a side-by-side comparison of HeLa cells treated with 10 μM ZS5 or ZP3 and 100 μM Zn(II)/pyrithione. ZP3

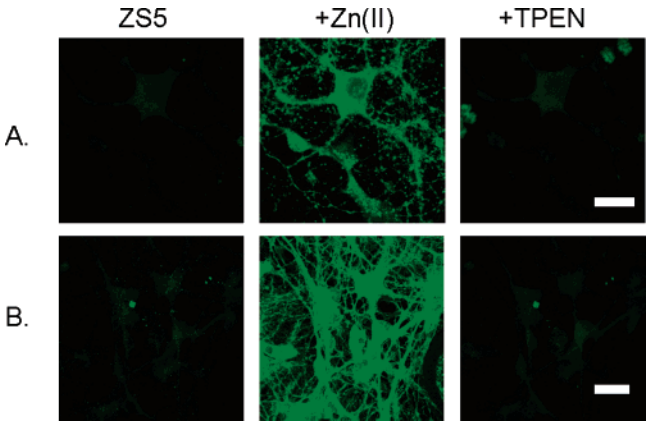

Figure 8. Response of ZS5 to exogenously added Zn(II) in primary cultures of hippocampal (row A) and dentate gyrus (row B) neurons. Left panels: Neurons were treated with 10 μM ZS5 for 30 min (37 °C, 5% CO_2), washed, and imaged. Middle panels: Fluorescence change observed 1 min (hippocampal neurons) or 5 min (dentate gyrus neurons) after addition of 50 μM Zn(II)/pyrithione (1:2 ratio). Right panels: Fluorescence decrease observed 1 min (hippocampal neurons) or 5 min (dentate gyrus neurons) after addition of 50 μM TPEN. The scale bars represent 25 μm.

exhibits punctate staining, similar to that previously reported for ZP1 in COS-7 cells,[47] whereas the ZS5 pattern is much more diffuse. Co-localization studies were therefore conducted in HeLa cells to determine where ZS5 and ZP3 reside, and representative images are provided in Figures S8 and S9. Treatment of HeLa cells with ZS5 (free or zinc-bound) and either Lysotracker or pGolgi-DsRed showed that this dye does not localize to either the lysosomes or the Golgi apparatus. Excellent co-localization of ZS5 and Mitotracker Red was observed, which establishes that ZS5 is sequestered in the mitochondria of healthy HeLa cells. In contrast, ZP3 shows excellent co-localization with pGolgi-DsRed and no overlap with the Lysotracker and Mitotracker markers, which establishes Golgi compartmentalization of this probe in HeLa cells.

The observation that Zn(II) sensors can be directed to different subcellular organelles as a result of structural modification is intriguing and potentially advantageous. Although subcellular compartmentalization of sensors has been described as problematic in the calcium sensor literature,[37] we believe that a clear understanding of sensor localization in the cell type under study will be beneficial for studying Zn(II) entry into and trafficking between certain organelles. Mitochondrial localization is relevant from the standpoint of Zn(II) toxicity, because rapid influx of Zn(II) into the mitochondria has been implicated in neuronal death.[28,31,85,86]

II. Response of ZS5 to Zinc in Primary Neuronal Cultures. We next focused our efforts on studying the behavior of ZS5 in primary neuronal cultures from pre- or postnatal rat. Two different types of neuronal cultures were used in this work.[87] Figure 8 exhibits representative images of both embryonic hippocampal and postnatal dentate gyrus neurons treated with ZS5 and exogenous Zn(II). ZS5 enters and is Zn(II)-responsive and reversible in both cell types.

A series of time-course experiments, in which cells were treated with 10 μM ZS5 and 50 μM Zn(II)/pyrithione and imaged over the course of 1−5 min, revealed that ZS5 responds to exogenously added Zn(II) more quickly in neurons than in other cell types, such as HeLa and COS-7. Whereas ca. 1 min of incubation was sufficient to observe full fluorescence enhancement in hippocampal neurons following treatment with 50 μM Zn(II)/pyrithione, ca. 5 min was required to observe complete turn-on in HeLa cells. We believe that this variation stems from the relative ability of the HeLa cells and neurons to internalize the Zn(II)/pyrithione complex. From a molecular standpoint, the difference in Zn(II)/pyrithione uptake might arise from the greater diversity of ligand, voltage, and resting cation membrane channels in neurons relative to HeLa cells.

We therefore questioned whether ZS5 would respond to Zn(II) on a faster time scale in vivo, a feature that is necessary for monitoring biological Zn(II) flux. Figure 9 shows time-series images of a hippocampal neuronal cell body treated with 10 μM ZS5 before and after addition of 50 μM 1:1 Zn(II)/pyrithione and 50 μM TPEN. The images were captured at ~2.4-s intervals and show that ZS5 responds to Zn(II) on this time scale in living cells. We chose this time interval because it allowed for real-time visualization of the signal on the computer screen without any image manipulation. Control studies show that pretreatment of the neurons with TPEN blocks any response of ZS5 to Zn(II)/pyrithione (data not shown). The origin of the fluorescence rise that occurs in the ca. 4 s following TPEN addition is unclear to us, but it is reproducible, and we have also observed this phenomenon in HeLa cells. The value of these experiments lies in their proof that ZS5 can respond to and release Zn(II) rapidly in a biological system, which points toward its utility for monitoring Zn(II) flux.

III. Effect of Glutamate on Exogenous Zinc Uptake. Treating cells with Zn(II)/pyrithione is essentially a brute force approach to generating a robust intracellular signal. Pyrithione appears to deliver Zn(II) indiscriminately throughout the cell. As a result, experiments that use Zn(II)/pyrithione have little physiological or pathophysiological significance. We were therefore motivated to investigate other routes of Zn(II) entry that may be relevant to neurobiological signaling.

The Zn(II)-containing synaptic vesicles in the mammalian hippocampus also house glutamate (E), an excitatory neurotransmitter, and both species are released into the synaptic cleft following exocytosis of vesicles at the pre-synaptic membrane. Given this association, it is reasonable to think that glutamate may modulate Zn(II) uptake into the post-synaptic neuron or other nearby cells. Several reports indicate that glutamate or kainate, a glutamate mimic, can trigger excessive intracellular accumulation of Zn(II) in cortical neurons.[86,88,89] We therefore co-treated ZS5-loaded hippocampal neurons with $ZnCl_2$ and glutamate (1:2 ratio, 50 μM zinc) and monitored the intracellular response by fluorescence microscopy. Figure 10 displays representative images, which show significantly different staining than that observed for neurons treated with Zn(II)/pyrithione. Fluorescence enhancements occur in several

(85) Sensi, S. L.; Yin, H. Z.; Carriedo, S. G.; Rao, S. S.; Weiss, J. H. *Proc. Natl. Acad. Sci. U.S.A.* **1999**, *96*, 2414−2419.
(86) Sensi, S. L.; Ton-That, D.; Weiss, J. H. *Neurobiol. Dis.* **2002**, *10*, 100−108.
(87) The hippocampal cultures were prepared from prenatal rat and contain cells from the entire hippocampus. The dentate gyrus cultures were prepared from postnatal rats and contain cells only from the dentate gyrus substructure. The dentate gyrus is the region of the hippocampus rich in Zn(II)-filled vesicles, which makes these cultures particularly interesting from the standpoint of Zn(II) neurobiology.
(88) Sensi, S. L.; Canzoniero, L. M. T.; Yu, S. P.; Ying, H. S.; Koh, J.-Y.; Kerchner, G. A.; Choi, D. W. *J. Neurosci.* **1997**, *17*, 9554−9564.
(89) Colvin, R. A.; Davis, N.; Nipper, R. W.; Carter, P. A. *J. Nutr.* **2000**, *130*, 1484S−1487S.

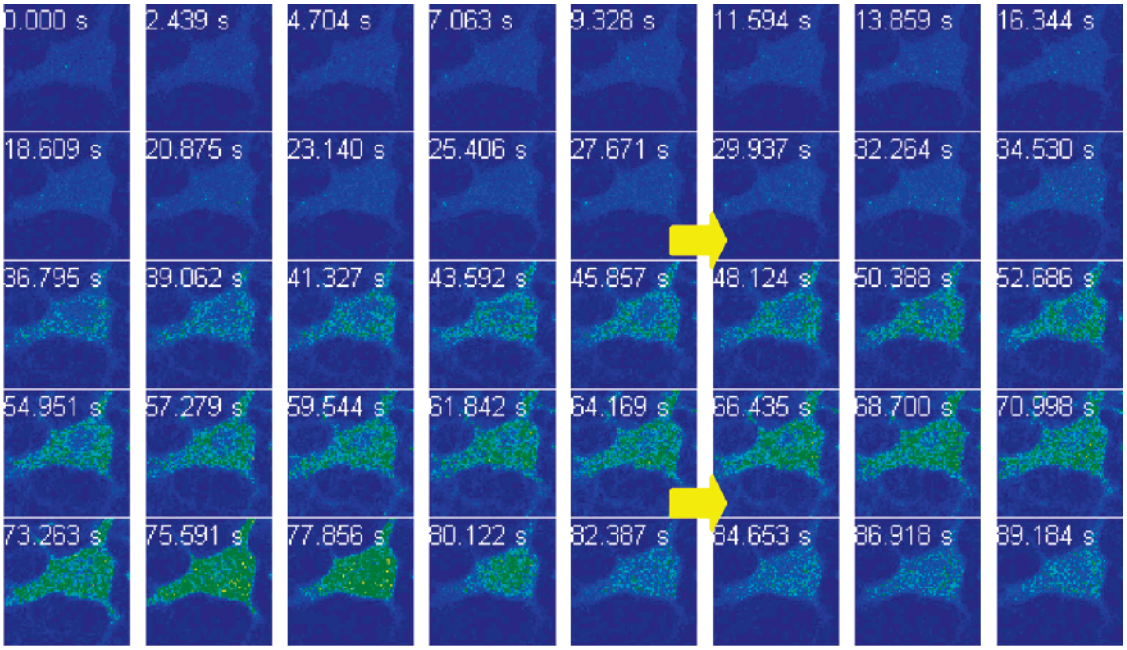

Figure 9. Time-lapse imaging of Zn(II) addition to primary cultures of hippocampal neurons (DIV 18) pretreated with 10 μM ZS5. The ZS5-treated cell was imaged (0−27.671 s); Zn(II)/pyrithione (50 μM, 1:1 ratio) was added during the image acquisition (29.937−34.530 s, top arrow), and a fluorescence rise is observed. An aliquot of TPEN (50 μM) was subsequently added during the data collection (66.435−70.998 s, bottom arrow), and a fluorescence decrease occurred at ca. 80 s.

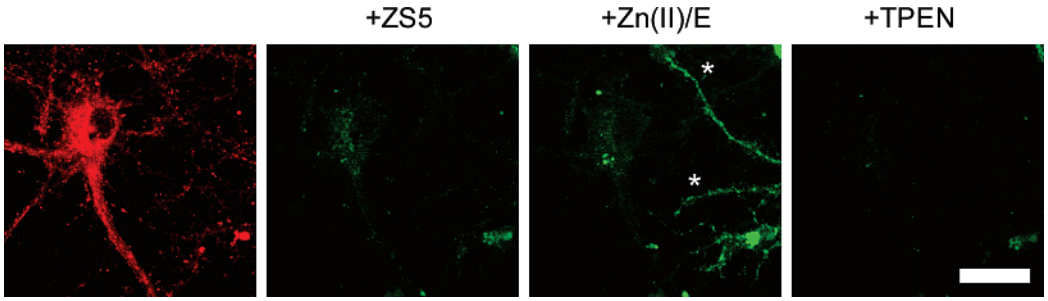

Figure 10. Uptake of exogenous Zn(II) by hippocampal neurons as a result of glutamate (E) treatment. Hippocampal neurons were treated with 10 μM ZS5 for 30 min (37 °C, 5% CO_2), washed, and imaged. The neurons were treated with 50 μM 1:2 Zn(II)/E and imaged 1 min following addition. A fluorescence rise occurs in a number of neuronal projections, labeled by asterisks. The fluorescence increase is reversed 1 min after addition of 50 μM TPEN. Lysotracker Red was used as the red marker in this experiment. The scale bar represents 25 μm.

neuronal projections 1 min after addition of the Zn(II)/E mix, and this rise persists for at least 5 min (Figure S11). The staining pattern consists of green dots that may be associated with dendritic spines and/or GABA synapses, although detailed co-localization studies must be conducted to address these possibilities. Control studies in which hippocampal neurons were treated with only $ZnCl_2$ (50 μM) showed no fluorescence change over a 5-min time frame, indicating that Zn(II) alone does not permeate the neuronal cell membrane over this time period (Figure S11). Additional control studies, in which the ZS5-loaded neurons were treated with glutamate (100 μM) for 5 min, also showed no fluorescence change (Figure S11). This experiment illustrates that extracellular glutamate modulates the uptake of Zn(II) into hippocampal neurons rapidly and at specific locales.

IV. Imaging Endogenous Zinc Mobilization with ZS5. We previously demonstrated that ZNP1, a ratiometric Zn(II) indicator with a sub-nanomolar K_d value for this metal ion, can detect endogenous Zn(II) mobilization in cultured COS-7 cells following SNOC treatment.[54] We therefore wondered whether ZS5 would illuminate Zn(II) mobilization in live cells following nitrosative stress. We chose neurons from the zinc-rich dentate gyrus region of the rat hippocampus for this experiment. Figure 11 shows a time-course experiment in which dentate gyrus neurons were loaded with 10 μM ZS5 and subsequently treated with SNOC. Significant fluorescence enhancement occurs in the neuron cell bodies and projections, and in surrounding glial cells, at ca. 3 min following SNOC addition, and the response maximizes at ca. 5 min.

To confirm that the observed changes in ZS5 fluorescence intensity observed after SNOC treatment are due to the NO-induced release of Zn(II) from native protein stores rather than to general cell toxicity, we monitored neuronal cell viability 30 min after SNOC application by employing established protocols for assaying cell death in dentate gyrus neurons.[78] In particular, we analyzed nuclear and dendritic morphology using DAPI (nuclear stain) and MAP2 (dendritic marker), as described in the Supporting Information. No statistically significant difference was observed in a comparison of nuclear morphology in untreated control and SNOC-treated cells (control, 96.7% survival; SNOC, 95.1% survival), and dendritic fragmentation, characteristic of apoptotic DG neurons, was not observed (Figure

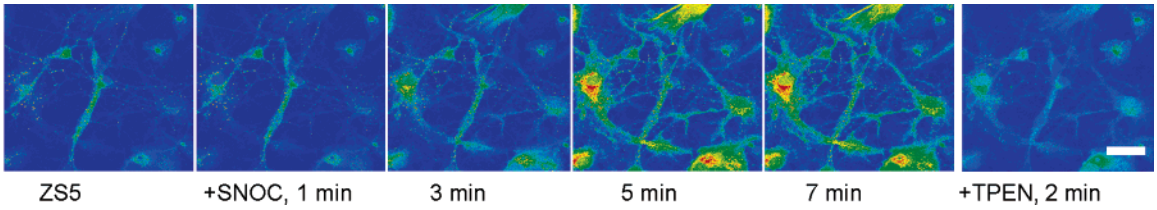

Figure 11. Imaging endogenous Zn(II) release in primary dentate gyrus neuronal cultures following nitrosative stress with ZS5. The cells were treated with 10 μM ZS5 (30 min, 37 °C, 5% CO_2), washed, and imaged. An aliquot of SNOC was added (final concentration = 1.5 mM), and the fluorescence change was recorded at 1-min intervals. Time points for 0, 1, 3, 5, and 7 min are shown above. The right-most panel shows the fluorescence decrease that occurred 2 min after addition of 200 μM TPEN. The scale bar indicates 25 μm.

Table 3. Cytotoxicity Data (HeLa, 24 h)[a]

	% cell survival		
	1 μM	5 μM	10 μM
ZP1	96 ± 2	68 ± 5	40 ± 6
ZP3	93 ± 4	73 ± 8	57 ± 13
ZS5	101 ± 1	87 ± 2	80 ± 4

[a] Cell viability was quantified by the MTT assay (mean ± SD).

S10). Together, these experiments establish that dentate gyrus neurons can release Zn(II) from native protein stores at concentrations observable with a low-micromolar affinity probe as a result of nitrosative stress.

Probe Cytotoxicity. Cytotoxicity is a potential side effect of a probe that must be controlled when dealing with living cells or tissues. Although we saw no evidence for cytotoxic effects during the experiments described in this work, these studies required relatively short time frames. We were therefore interested in studying the possible consequences of a more extended sensor treatment on cell viability. To date, we have conduced cytotoxicity assays only in HeLa cells, but this information should prove useful in the design of experiments requiring other cell lines. Table 3 lists the cell viability data for HeLa cells treated with ZP1, ZP3, and ZS5 as quantified by the MTT assay, an established method of probing apoptotic cell death. Corresponding bar graphs are given in Figure S12. These data show that HeLa cells show ~100% viability following 24-h treatment with 1 μM ZP1, ZP3, or ZS5. Higher sensor concentrations result in decreased cell survival, with 80% ± 4% viability observed following 24-h treatment with 10 μM ZS5. These cytotoxicity tests indicate that sub- and low-micromolar concentrations of ZP and ZS5 are essentially nontoxic over at least a 24-h period and can safely be used for biological studies that require prolonged sensor treatment.

Summary

Turn-on fluorescent Zn(II) sensors of the Zinspy family give improved dynamic range by substituting thioethers with thiophene groups, which affords lower background fluorescence and bright Zn(II) complexes. These sensors exhibit a number of advantageous features. From a chemical perspective, they provide (i) dissociation constants in the low micromolar range, (ii) fast Zn(II) association rates comparable to those observed for Zn(II) sensors employing the DPA chelate but with more rapid Zn(II) dissocation, and (iii) improved selectivity for Zn(II) compared to the parent ZP and ZS compounds. Our studies demonstrate that fluorescein halogenation is a general strategy for modulating not only photophysical but also metal-binding properties of fluorescent metal ion sensors. From the standpoint of biological imaging, ZS5 is a robust and versatile tool for illuminating Zn(II) uptake and mobilization in living cells, including neurons. Mitochondrial probe localization occurs for ZS5 in HeLa cells, in contrast to the Golgi localization of ZP3, demonstrating that ligand modifications can direct fluorescein-based sensors to specific locales. Glutamate-dependent Zn(II) entry into embryonic hippocampal neurons was visualized, as was Zn(II) release from native protein stores in dentate gyrus neurons. We anticipate that ZS5, alone or in combination with high-affinity Zn(II) probes such as ZP3, will be useful for studies of Zn(II) physiology and pathology in a variety of contexts.

Acknowledgment. This work was supported by Grant GM65519 from the National Institute of General Medical Sciences. Spectroscopic instrumentation at the MIT DCIF is maintained with funding from NIH Grant 1S10RR-13886-01 and NSF Grants CH3-9808063, DB19729592, and CHE-9808061. M.S. is an investigator of the Howard Hughes Medical Institute. E.M.N. thanks the Whitaker Health Science Fund for a graduate fellowship and Dr. D. Song for assistance with collecting the X-ray data.

Supporting Information Available: Tables S1 and S2, Scheme S1, Figures S1−S12, CIF files, experimental details for X-ray crystallographic modeling studies and cytotoxicity assays in dentate gyrus neurons, representative ^{1}H NMR spectra, and IR spectral data for all probes. This material is available free of charge via the Internet at http://pubs.acs.org.

JA065759A